Eur Biophys J (2007) 36:661–668
DOI 10.1007/s00249-007-0141-7

ORIGINAL PAPER

Mechanical and structural properties of in vitro neurofilament hydrogels

S. Rammensee · P. A. Janmey · A. R. Bausch

Received: 13 November 2006 / Revised: 24 January 2007 / Accepted: 29 January 2007 / Published online: 6 March 2007
© EBSA 2007

Abstract Neurofilaments belong to the class of cytoskeletal intermediate filaments and are the predominant structural elements in axons. They are composed of a semiflexible backbone and highly charged anionic sidearms protruding from the surface of the filaments. Here, the rheology of in-vitro networks of neurofilaments purified from pig spinal cord was determined. The mechanical properties of these networks are qualitatively similar to other hydrogels of semiflexible polymers. The low-deformation storage modulus $G'(\omega)$ showed a concentration (c) dependence of $G' \sim c^{1.3}$ that is consistent with a model for semiflexible networks, but was also observed for polyelectrolyte brushes. A terminal relaxation was not observed in the frequency range investigated (0.007–5 Hz), supporting the notion that sidearms act as cross-links hindering slip between filaments on a time scale of many minutes. The mesh size distribution of the network was measured by analysis of Brownian motion of embedded beads. The concentration dependence of the mesh size follows the same power law behaviour as found for F-actin networks, but shows a significantly wider distribution attributable to the smaller persistence length of neurofilaments. The attractive interaction between filaments is increased by addition of Al^{3+} ions resulting in a reduction of the linear response regime from strains bigger than 80% to less than 30%.

S. Rammensee · A. R. Bausch (✉)
Biophysik (E22), Technische Universitaet Muenchen,
James-Franck-Strasse, 85747 Garching, Germany
e-mail: abausch@ph.tum.de

P. A. Janmey
Institute for Medicine and Engineering,
University of Pennsylvania,
1010 Vagelos Labs, 3340 Smith Walk,
Philadelphia, PA 19104, USA

Introduction

Shape and mechanical properties of cells are defined by the cytoskeleton, a biopolymer scaffold which can be adjusted dynamically to the needs of the cell. The cytoskeleton is formed by F-Actin, microtubules and intermediate filaments (IF). Since many important features of cells, such as translocation, resistance to mechanical stresses, transport of vesicles, adhesion to substrates and also cell division depend strongly on the physical features of the biopolymers that compose the cytoskeleton, a better understanding of their properties and interactions is needed. While the mechanical properties of F-actin and their foundation in the physics of semiflexible polymer networks have been studied in great detail, and in vitro systems with increasing complexity have been constructed (for a recent review see e.g. Bausch and Kroy 2006), much less is known of the physics of intermediate filaments, such as desmin, vimentin, or neurofilaments. Intermediate filaments show a much smaller persistence length (Dalhaimer et al. 2005; Hohenadl et al. 1999), ~500 nm compared to 17 μm for F-Actin.

Interestingly, for the intermediate filament vimentin it has been shown that subunits can glide axially against each other (Guzman et al. 2006), thus rendering the concept of persistence length more complex than for a uniform cylindrical filament. The major consequence for modelling such IF networks is that the bending modulus of the individual filaments becomes a function

of the filament length, comparable to actin bundles or microtubules (Bathe et al. 2006; Claessens et al. 2006; Pampaloni et al. 2006). To complicate the matter further some of the intermediate filaments, such as neurofilaments, have highly charged side arms, which introduce a significant interaction between the filaments in the networks.

Neurofilaments (NF) are the most abundant cytoskeletal filaments in axons. They fill most of its diameter and are proposed to provide structural stability. NFs are formed by three polypeptides: NF-H (high), NF-M (medium) and NF-L (low). In-vivo NF proteins are bundled into filaments, where the alpha-coil parts of the NF proteins form a semi flexible backbone ($l_p \approx 500$ nm) and the C-terminal ends of NF-H and NF-M protrude as unfolded side arms with a length of about 70 nm that depends on their state of phosphorylation and ionic conditions (Aranda-Espinoza et al. 2002). Interactions between NF sidearms are thought to mediate connections between NFs with each other and with other cytoskeletal filaments (Chen et al. 2000), and alterations of the sidearms have been reported to alter the mechanical properties of neurofilament gels (Gou et al. 1998; Leterrier et al. 1996; Leterrier and Eyer 1987). These interactions could either result in cross-linking the individual filaments with each other or in introducing a repulsive interaction by a polymer cushion effect between the filaments (Kumar et al. 2002a; Mukhopadhyay et al. 2004). The interaction between filaments is greatly increased by Al^{3+} ions which results in altered mechanical properties and structure of the hydrogels (Leterrier et al. 1992).

In this paper, in-vitro networks of neurofilaments from pig spinal cord were characterised with rheological methods and multi particle tracking. Combined data of rheology and network structure of in vitro neurofilament networks provide evidence for the role of interactions between the filaments in determining the mechanical network properties.

Materials and methods

Protein preparation

Neurofilaments were prepared from pig spinal cords (Municipal Slaughterhouse, Munich, Germany), based on a previously published method for purification from bovine material (Leterrier et al. 1996) with some changes to account for different tissue properties: the crude NF pellet was resuspended in five times higher volume of buffer than in the preparation of bovine spinal cord. This is to take into account the higher amount of sedimentable membranes in pig tissue compared to bovine tissue (J. F. Leterrier 2005, personal communication).

Protein purity was controlled by SDS-PAGE, and concentration was determined by Bradford assay, with BSA as standard. Neurofilaments in Reassembly Buffer (RB, 0.1 M MES, 1 mM EGTA, 1 mM $MgCl_2$) with 0.8 M sucrose were stored at –80°C. One hour before rheological experiments, samples were thawed; samples were vortexed three times for 30 s, with resting on ice for 20 s between each vortexing step immediately before rheological experiments (Leterrier et al. 1996).

The phosphorylation state of the neurofilaments was not altered or controlled specifically. The purity of the preparation can be seen on SDS-PAGE (Fig. 1), where no evidence for the presence of cross-linking proteins in the sample is found.

Rheology

A commercial rheometer (Physica MCR 301, Anton Paar, Ostfildern, Germany) equipped with a 25 mm cone and plate geometry (CP25-2), with a cone angle of 2° and a truncation at the tip of 50 µm, corresponding to the set gap size, was used. The temperature of the lower plate was controlled by a Peltier element; measurements were conducted at 25 or 35°C.

Oscillatory experiments were conducted in strain controlled mode. A sinusoidal strain $\gamma(t) = \gamma_0 \sin \omega t$ was applied to the sample and the resulting stress $\sigma(t) = \sigma_0/\gamma_0 \cos \delta$ was measured. The storage modulus is then defined as $G' = \sigma_0/\gamma_0 \cos \delta$ and the loss modulus as $G'' = \sigma_0/\gamma_0 \sin \delta$. Transient experiments were also performed in strain controlled mode; in this case the deformation was increased linearly over time, resulting in a constant strain rate.

Salt concentrations and the total protein concentration were adjusted by adding $MgCl_2$ or $AlCl_3$ solutions and RB buffer. Samples were mixed gently and pipetted onto the lower plate of the rheometer, which

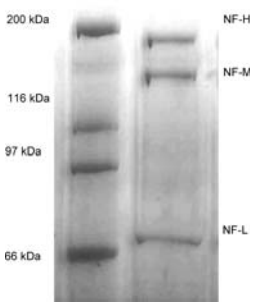

Fig. 1 SDS-PAGE of neurofilaments. SDS-PAGE of neurofilaments purified from pig spinal cord. *NF-H*, *NF-M* and *NF-L* are easy to distinguish in the right column and no cross-linking proteins are evident. Molecular weight markers are shown in left lane

was set to a temperature of 35°C. The upper plate was initially kept at room temperature.

In order to study the nonlinear viscoelastic response of the material, a 'prestress' was applied to the samples onto which a small oscillatory stress $\delta\sigma$ was superposed. The small oscillatory stress yields a small oscillation with amplitude $\delta\gamma$. The differential storage modulus is then defined as $K'(\sigma_0) \sim \delta\sigma/\delta\gamma$ at a given σ_0 (Gardel et al. 2004). In the next step, the prestress was increased and again a small oscillatory stress was superimposed.

Mesh size determination

Polystyrene beads (Interfacial Dynamics, Portland, USA) were coated with poly-ethylene-glycol (PEG) (Valentine et al. 2004). The diameter of the beads used was 830 nm for 4 and 2 mg/ml neurofilament samples, and 1,200 nm for 1 and 0.5 mg/ml samples. Neurofilament samples were mixed with PEG-coated beads, placed into a custom-built sample chamber and allowed to incubate in a water bath at 35°C for 2 h. The thermal motion of beads far from the walls of the chamber was recorded using a Zeiss Axiovert Microscope with a 40 × Objective and a digital camera (OrcaEr, Hamamatsu, Germany). Trajectories were obtained using the Program OpenBox (Schilling et al. 2004) and the mean-squared displacement (MSD) $\langle \Delta r^2(\tau) \rangle = \left\langle |r(t+\tau) - r(t)|^2 \right\rangle$ was calculated. The MSD of spherical probes embedded in the network is directly related to the mesh size of the network, if two conditions are fulfilled: (a) for short lag times τ, the slope of MSD over τ is equal to 1, which is characteristic for free diffusion, (b) for long τ, the MSD reaches a plateau. In this case, the mesh size is given by the sum of the plateau $\sqrt{\langle \Delta r^2(\tau) \rangle}$ at long times and the bead diameter. In order to measure mesh size correctly, the bead diameter was adjusted to the actual mesh-size experimentally, until MSD(τ) curves showed the required properties.

Results

In vitro networks of neurofilaments were first studied by determining the concentration dependence of the elastic moduli. Initially, directly after pipetting the neurofilament solution onto the rheometer an increase of the storage modulus for about 1 h was observed until a stable equilibrium value for the elastic modulus was reached. This initial increase in the elastic properties is attributable to the onsetting gelation of neurofilaments upon addition of 5 mM $MgCl_2$ (Leterrier and Eyer 1987). The storage modulus G' was almost frequency independent below 1 Hz for all measured concentrations, indicative for a cross linked gel (Fig. 2a) (Rubinstein and Colby 2004). At all times the loss modulus remained almost constant and an order of magnitude lower than the storage modulus. The concentration dependence of the equilibrated elastic modulus G' was determined at 0.5 Hz, showing a concentration (c) dependence of $G' \sim c^{1.3}$ (Fig. 2b).

From multiparticle tracking we determined that the mesh size of neurofilament networks depends on the concentration by $\xi \sim c^{-0.44}$ (Fig. 3a). This is in good agreement with a purely geometric prediction for networks, where the mesh size ξ depends on the concentration c as $\xi \sim c^{-0.5}$ (Schmidt et al. 1989). However, the distribution of mesh sizes (Fig. 3b) is much broader (full width half maximum, FWHM ~ 4 μm) than observed for actin networks, where a distribution with FWHM of approximately 0.3 μm was observed even for low (0.4 mg/ml) F-actin concentrations (Tharmann et al. 2006). The weak concentration dependence confirms that indeed the mesh sizes are probed rather than local moduli, which would result in much stronger concentration dependence.

In a next set of experiments we studied the nonlinear behaviour of the neurofilament networks (Fig. 4) by determining the differential storage modulus K' by a prestress method, which is applicable here as the networks are predominantly elastic in their response (Gardel et al. 2004). The linear response regime extends up to a critical prestress, which value depends on the concentration studied. Above σ_{crit} the nonlinear response of the gel sets in and a stiffening of the network is observed where K' follows a power-law behaviour $K' \sim \sigma_0^x$ with an exponent $0.8 < x < 1$ for all measured samples. When the prestress exceeds a critical value $\sigma_{0,crit}$, the sample fails and ruptures. $\sigma_{0,crit}$ increases with protein concentration (Fig. 4). In the inset of Fig. 4, the data are rescaled to the storage modulus in the linear regime. The curves superimpose, indicating that principally the same behaviour is observed in all of them.

At a given neurofilament concentration (c_{NF} = 0.5 mg/ml) electrostatic screening effects were studied by varying the sodium chloride concentration in the solution. By decreasing the electrostatic screening lengths κ^{-1} from 0.6 to 0.3 nm the absolute value of the elastic plateau modulus was decreased by a factor of about 3 (Fig. 5).

The presence of aluminium ions increased the low-deformation dynamic storage modulus G' (Fig. 6a) at

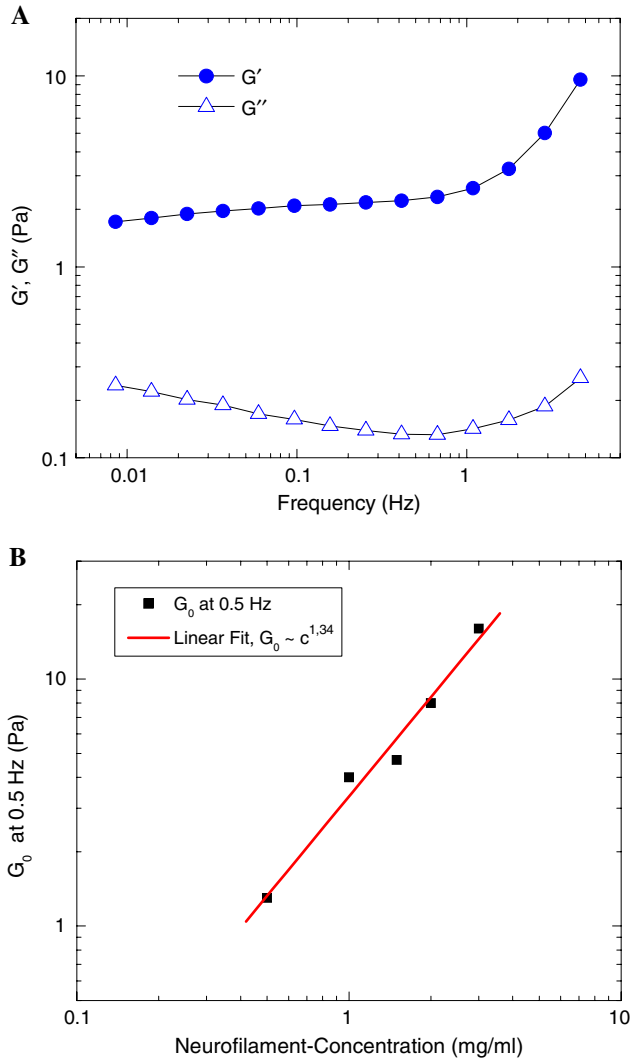

Fig. 2 **a** Frequency dependence of the storage modulus. Typical frequency dependence of storage (G') and loss moduli (G'') for neurofilament networks (shown here for 0.8 mg/ml neurofilament concentration). G' shows a plateau over a wide frequency range below 1 Hz, indicating that no slip between the filaments is possible and that the material is a gel-like solid. **b** Concentration dependence of the storage modulus. Plateau storage modulus at 0.5 Hz for neurofilament networks for protein concentrations of 0.5–4 mg/ml. Values shown here were measured after 1 h at 35°C. The storage modulus follows a power-law behavior of $G' \sim c^{1.3}$ for the investigated neurofilament concentrations. The observed concentration dependence is in accordance with a 'Tube Model' for purely entangled semiflexible biopolymer networks, predicting a scaling of the storage modulus $G' \sim c^{7/5}$

0.5 Hz significantly, compared to the samples in the presence of only magnesium ions as a control. Also, we found that addition of Al^{3+} results in a higher shear modulus $G = \sigma/\gamma$ which denotes a stiffer behaviour of the networks. This can be seen in the increase of the initial slope in Fig. 6b in the presence of aluminium ions. Also, a shift of the yield point towards much smaller deformations is observed in rotation mode experiments (Fig. 6b). One should be aware that the given concentrations for $AlCl_3$ do not accurately reflect the concentrations of Al^{3+} ions in the solution, as some of the aluminium complexes to $(AlCl_4)^-$ also.

Discussion

The mechanical properties of neurofilament networks require contributions of both the polyelectrolyte sidearms as well as the semiflexible backbone with the possibly length dependent persistence length of the individual filaments. Hence, it cannot be expected that existing theoretical models are able to describe the mechanical properties of such networks.

The observed concentration dependence (Fig. 2b) of the storage modulus for neurofilaments networks is of the order of magnitude that is expected for biopolymer networks in this concentration range (Bausch and Kroy 2006; Hinner et al. 1998; Mackintosh et al. 1995; Tharmann et al. 2006). The power-law dependence that was observed, $G' \sim c^{1.3}$, corresponds very well with a model developed for purely entangled semiflexible polymers (Hinner et al. 1998; Isambert and Maggs 1996). Models for cross-linked semiflexible polymers predict a scaling exponent larger than 2, which is clearly different from the presented experimental results (Mackintosh et al. 1995).

However, the absence of a decrease of the storage modulus at low frequencies (Fig. 2a) in the accessible frequency range indicates that the filaments can hardly freely flow on the time scales measured (0.2–150 s). Thus, the frequency spectrum of the studied reconstituted neurofilaments networks resembles that of a cross-linked network rather than a purely entangled network.

This discrepancy suggests that the assumptions of the existing models for semiflexible filament networks are not fulfilled by neurofilament networks. Both the tube model for entangled semiflexible polymers (Hinner et al. 1998; Isambert and Maggs 1996) as well as the single filament stretching model (Mackintosh et al. 1995) assume the persistence length to be larger than the mesh size of the gel ($1_p > \xi$). However, our measurements with multi-particle tracking show, that the mesh size of neurofilament gels (Fig. 3a) is larger than their persistence length ($\xi > 1_p$) of approximately 500 nm (Dalhaimer et al. 2005).

Mesh sizes for neurofilament gels scale as ξ [μm] = 5 · ($c^{-0.44}$ [mg/ml]). For F-actin, a mesh size dependence of ξ [μm] = 0.3 · ($c^{-0.5}$ [mg/ml]) has been observed (Schmidt et al. 1989). Taking into account

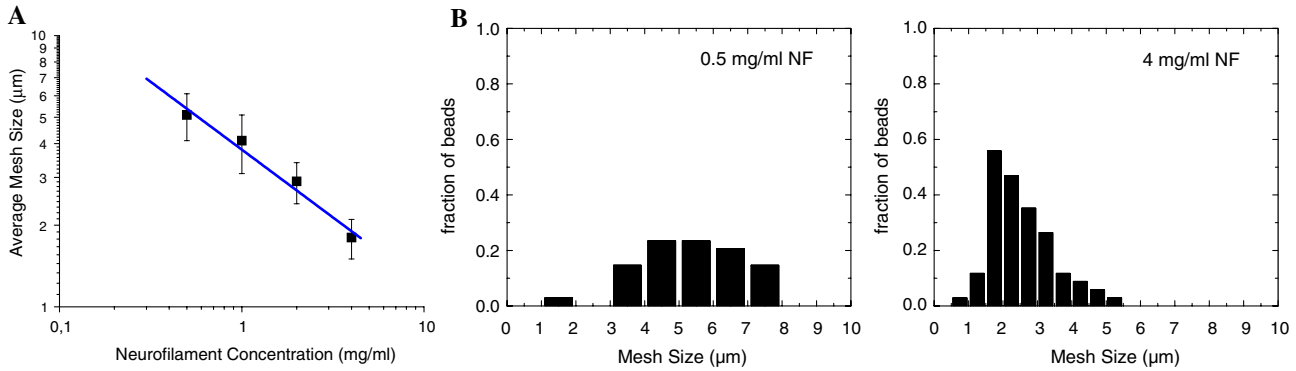

Fig. 3 Mesh size distribution in neurofilament hydrogels. **a** Mesh size of neurofilament networks as measured by the Brownian motion of beads of the same order of magnitude as the 'pores' (see Materials and methods section). Mesh size ξ scales with the concentration c as $\xi \sim c^{-0.44}$, indicated by the *line*. Geometrical considerations for stiff rods lead to a square root dependence, which is close to the observed behavior. **b** Mesh size distribution for two concentrations of neurofilaments (0.5 and 4 mg/ml). The mesh size distribution is wider and has a center at larger values for the low protein concentration. At high protein concentration, the distribution is narrower and the mean mesh size is lower

the stoichiometry of NF-L:NF-M:NF-H of 7:3:2 and the assumption that every section of the filament consists of eight tetramers, a mass of approximately 64 kDa per nm can be calculated (Alberts et al. 2002; Janmey et al. 2003). This calculated mass per nm is almost four times higher than for F-Actin. Thus, the observed mesh sizes are smaller than what would be expected considering that the mesh size is directly connected to the total length of filaments per volume. This can be a result of the persistence length being smaller than the mesh size. The width of the mesh size distributions (Fig. 3b) is also much wider than observed in F-actin networks, which can be attributed to the additional space accessible for the test particles by fluctuations of the filaments, which are expected to be larger due to the smaller persistence length.

In the nonlinear viscoelastic regime, our results on neurofilaments vary from what has previously been reported for cross-linked actin networks (Gardel et al. 2004; Tharmann et al. 2007). The slope of the differential elastic modulus K' is significantly reduced in the more flexible NF networks. It is as yet not understood whether this effect is caused by flexibility in the backbone, axial sliding, or by different interaction potentials between the filaments than in F-actin networks. Recent AFM experiments (Guzman et al. 2006) suggest that axial sliding of the building blocks of vimentin IFs is possible. Thus, intermediate filaments presumably have to be regarded more like elastic cables and this would clearly lead to a different nonlinear rheological behavior for intermediate filaments than for axially firm F-actin filaments.

The effect of higher monovalent salt concentrations (Fig. 5) on the elastic modulus of the gels remains to be understood on a molecular basis. The origin of the decrease in the storage modulus is unclear, but cannot be attributed directly to electrostatic screening, since the electrostatic screening length κ^{-1} is only about 0.6 nm even for the solution without additional sodium chloride and falls to 0.3 nm for the high salt concentrations. However, interactions between biopolymers are known to be highly salt dependent. Recent experiments on F-Actin showed a very sensitive dependence of the elastic properties on the salt concentration (Semmrich 2007).

Three-valent ions are thought to increase significantly the interaction between NF sidearms (Shea and Beermann 1994). Aluminium is reported to induce a neurofibrillary pathology similar to that seen in neurological diseases such as amyotrophic lateral sclerosis, dementia after renal dialysis and other peripheral neuropathies. In neurons, aluminium exposure for various periods results in the formation of abnormal bundles (Langui et al. 1988, 1990). Both the observations in rheological measurements as well as TEM micrographs (data not shown) support the notion that neurofilament sidearms interact more strongly with each other in the presence of Al^{3+}, as previously shown by viscosimetry and TEM (Langui et al. 1988, 1990; Leterrier et al. 1992). In the rheological data, aluminium alters the mechanical properties of the network drastically, causing a much stiffer and brittle behaviour compared to networks without aluminium ions (Fig. 6). In the transient response, the yield point is shifted to lower strain values, while the stress that has to be exerted to the sample to reach a certain strain is significantly higher in the presence of aluminium ions. Thus the sidearms of neighbouring filaments seem to interact with the same Al^{3+} ion, which then reduces slipping of the filaments against each other and leads to the

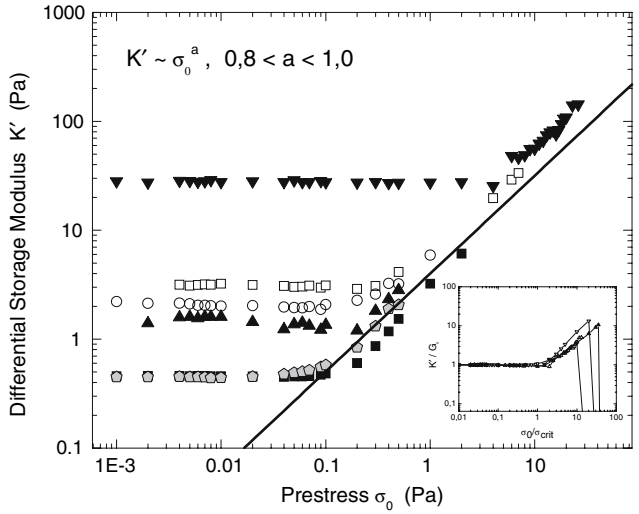

Fig. 4 Differential elastic modulus shows transition from linear to non-linear viscoelastic response. Differential storage modulus K' as a function of prestress σ_0. Each symbol type stands for one concentration of neurofilaments: *filled square* and *filled pentagon* 0.2 mg/ml; *filled up triangle* 0.5 mg/ml; *circle* 0.8 mg/ml; *square* 1 mg/ml; *filled down triangle* 5 mg/ml. K' remains constant for each sample up to a certain critical prestress. At prestresses larger than the critical prestress, K' increases following a power-law dependence of $K' \sim \sigma_0^x$, with $0.8 < x < 1$ in our experiments. The *black line* is a function $K' \sim \sigma_0^{0.9}$ to guide the eye. This behavior shows a significantly lower exponent than reported for F-actin networks in similar experiments. *Inset*: Superposition of all of the curves in the larger figure. K' is normalized to the value at low prestress, and the prestress σ is normalized to the critical shear stress σ_{crit}, the onset of the nonlinear behavior. All of the curves fall on the same master curve, indicating that the same rheological behavior is observed independent of the filament concentration

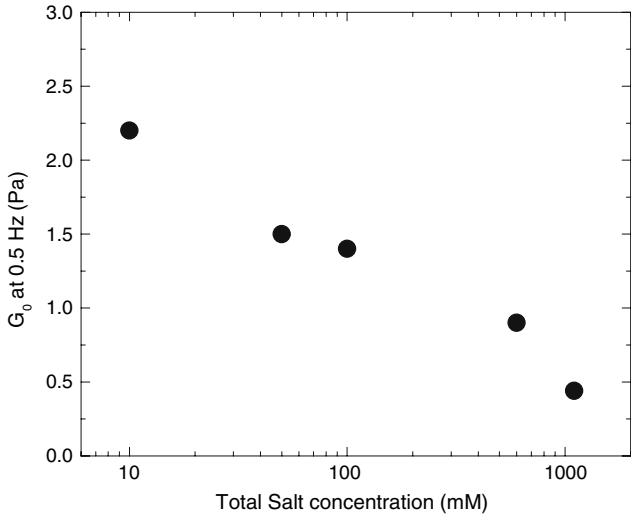

Fig. 5 Influence of monovalent salts on the storage modulus. Storage Modulus for samples of same neurofilament protein concentration (0.5 mg/ml), but with different total salt concentration. Salt concentration was adjusted by the addition of NaCl. The storage modulus is significantly lower in the presence of high concentrations of salt

observed reduction in the strain to yield (Leterrier et al. 1992).

The structure and apparent function of neurofilaments in the axon resemble, in some respects, those of aggrecan aggregates in cartilage. Aggrecan aggregates are brush-like polyelectrolyte polymers formed by binding of aggrecan subunits to a hyaluronan core via linking proteins. The sidechains are negatively charged, and the structure of the whole complex, as well as interactions with its neighbours are highly dependent on ionic strength, giving rise to a neutral brush regime, an osmotic brush regime and an ionic brush regime with different mechanical properties of the resulting gel (Meechai et al. 2002). A strong initial increase of the storage modulus ($G' \sim c^2$) around the overlap concentration and a much weaker increase for higher concentrations ($G' \sim c^{0.6}$) was found for aggrecan networks (Meechai et al. 2002). The latter scaling was attributed to forced deswelling of the subunits. Our experiments with neurofilament networks were done at approximately physiological ionic strength, where we found a constant scaling of the storage modulus, but the concentration range that was accessible in our experiments was much smaller. It is possible that the observed scaling for neurofilaments ($G' \sim c^{1.3}$) is observed in a transition between two concentration regimes. Also the compliance of NF gels in the nonlinear regime seems to be similar to the reported behaviour of aggrecan aggregates (Meechai et al. 2001).

Our data on neurofilament networks suggest that they behave on one side very similar to actin networks, as is shown by the pronounced concentration dependence of the storage modulus of our neurofilament networks and by the concentration dependence of the mesh size. On the other hand the frequency spectrum and the relaxation spectra of neurofilaments vary from those of purely entangled F-actin and share more features with cross-linked F-actin networks. This is attributable to the presence of charged sidearms that protrude from the neurofilaments, a structure with no direct analogue in F-actin networks without cross-linking molecules. However, the effect of flexible cross linking molecules with low off rates in actin networks could mimic the interactions of the sidearms, which could possibly relate to the observed (Fig. 2a) small increase at long times in G'' (Tharmann et al. 2007).

It has been discussed whether the interactions between neurofilament sidearms are repulsive or attractive (Gou et al. 1998; Janmey et al. 2003; Kumar and Hoh 2004; Kumar et al. 2002b; Mukhopadhyay et al.

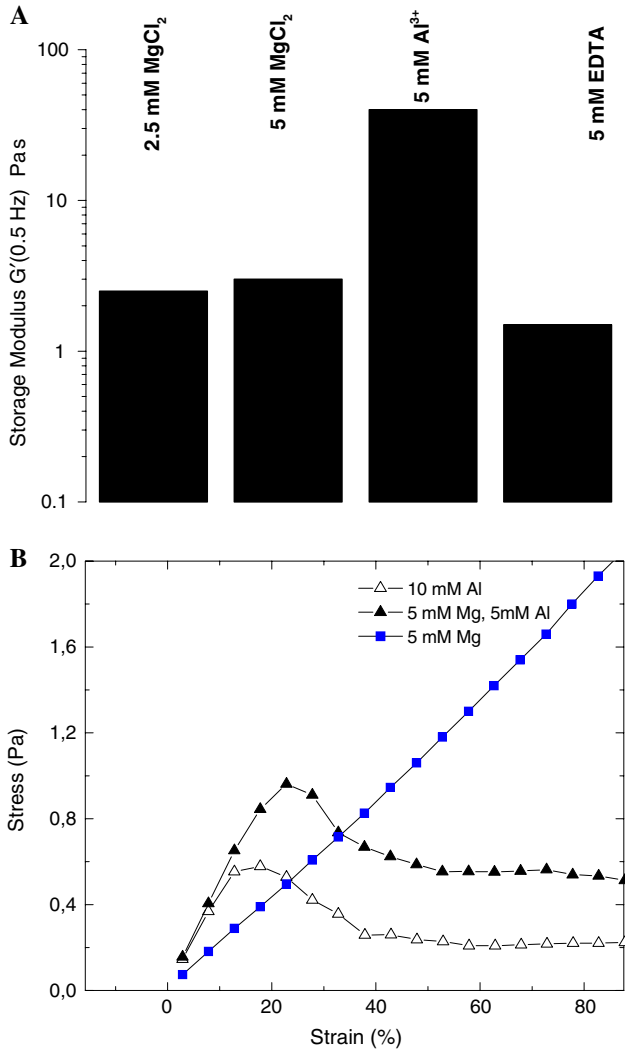

Fig. 6 Aluminium ions lead to a brittle behavior of neurofilament Hydrogels. **a** The presence of aluminium ions significantly increase the low-deformation dynamic storage modulus $G'(\omega)$ at 0.5 Hz, compared to the samples in the presence of only magnesium ions. **b** Stress/strain curve of a transient experiment. Strain is increased linearly with time resulting in a constant shear rate. The control sample with only Mg^{2+} (*squares*) shows a linear behavior until deformations of about 100%. In the presence of Al^{3+} Ions, the yield point shifts to much lower deformations (around 30%) and the initial slope of the stress curve is steeper than in the control sample, indicating an increased modulus $G(t)$ (*black triangles*). Higher concentrations of Al^{3+} increase this effect, especially lowering the yield point (*open triangle*)

2004). Our data suggest an attractive interaction which leads to the strongly cross linked behaviour of the network. This is supported by the fact that the presence of aluminium ions increases the stiffness of the network. An alternative explanation of the observed cross-linking effects might be due to as yet unidentified cross-linking proteins that were not removed during purification of neurofilaments. However, considering the purity of the gel this possibility appears unlikely. Additionally, rheological experiments in rotational mode and in the absence of aluminium ions show a very long linear behaviour, which could not be explained by a tightly cross-linked network.

Conclusion/summary

We present a set of experimental results on the microstructure and rheology of neurofilament networks which allows for the development of models of the underlying polymer physics. Network architecture of neurofilament shows a wide distribution of mesh sizes, which can be attributed to the change in the length scale of the filament stiffness compared to F-actin and consequential strong curvature of neurofilaments on the length scale of the test particle. The mesh size distribution is thus smeared out over the whole area that is made accessible by the filament fluctuations.

While frequency-dependent measurements indicate that no slip between the filaments occurs, resulting in a gel-like behaviour, the concentration dependence does not follow any of the scaling laws proposed for cross-linked semiflexible networks (Head et al. 2003; Kroy and Frey 1996; Mackintosh et al. 1995; Wilhelm and Frey 1996).

In the nonlinear viscoelastic regime, the observed differential storage modulus was different from that reported for tightly cross-linked F-actin networks. It is now possible to compare in detail rheological and structural data of neurofilament and other IFs networks to the relative abundance of data available for F-actin networks. It will only be possible to distinguish network versus single filament contributions to the mechanical properties of a semiflexible network by comparing the properties of networks of different filament types and by taking into account what is known about the respective filaments from single filament experiments. Concerning the discussion whether the interaction between neurofilaments is repulsive or attractive, our results indicate that there is a strong interaction between neurofilaments, leading to properties similar to a cross linked gel rather than a purely entangled semiflexible network (Janmey et al. 2003; Kumar et al. 2002a). Therefore, an attractive interaction between neurofilaments should also be taken into account when one models the interaction of the filaments in axons.

Acknowledgments This work was supported by the DFG (SFB–413). The authors thank J.F. Letterier for helpful discussions. S.R. was supported by the CompInt program of the ENB Bayern.

References

Alberts B, Johnson A, Lewis J, Raff M, Roberts K, Walter P (2002) Molecular biology of the cell, 4th edn. Garland Science, New York, p 924

Aranda-Espinoza H, Carl P, Leterrier JF, Janmey PA, Discher DE (2002) Domain unfolding in neurofilament sidearms: effects of phosphorylation and ATP. FEBS Lett 531:397–401

Bathe M, Heussinger C, Claessens C, Bausch A, Frey E (2006) Mechanics of nanofiber bundles. q-bio.BM/0607040

Bausch AR, Kroy K (2006) A bottom-up approach to cell mechanics. Nat Phys 2:231–238

Chen JG, Nakata T, Zhang ZZ, Hirokawa N (2000) The C-terminal tail domain of neurofilament protein-H (NF-H) forms the crossbridges and regulates neurofilament bundle formation. J Cell Sci 113:3861–3869

Claessens MMAE, Tharmann R, Kroy K, Bausch AR (2006) Microstructure and viscoelasticity of confined semiflexible polymer networks. Nat Phys 2:186–189

Dalhaimer P, Wagner O, Leterrier JF, Janmey PA, Aranda-Espinoza H, Discher D (2005) Flexibility transitions and looped adsorption of wormlike chains. J Poly Sci B 43:280–286

Gardel M, Shin J, MacKintosh F, Mahadevan L, Matsudaira P, Weitz D (2004) Elastic Behavior of cross-linked and bundled actin networks. Science 304:1301–1305

Gou JP, Gotow T, Janmey PA, Leterrier JF (1998) Regulation of neurofilament interactions in vitro by natural and synthetic polypeptides sharing Lys-Ser-Pro sequences with the heavy neurofilament subunit NF-H: Neurofilament crossbridging by antiparallel sidearm overlapping. Med Biol Eng Comput 36:371–387

Guzman C, Jeney S, Kreplak L, Kasas S, Kulik AJ, Aebi U, Forro L (2006) Exploring the mechanical properties of single vimentin intermediate filaments by atomic force microscopy. J Mol Biol 360:623–630

Head D, Levine A, MacKintosh F (2003) Distinct regimes of elastic response and deformation modes of cross-linked cytoskeletal and semiflexible polymer networks. Phys Rev E 68:061907

Hinner B, Tempel M, Sackmann E, Kroy K, Frey E (1998) Entanglement, elasticity, and viscous relaxation of actin solutions. Phys Rev Lett 81:2614–2617

Hohenadl M, Storz T, Kirpal H, Kroy K, Merkel R (1999) Desmin filaments studied by quasi-elastic light scattering. Biophys J 77:2199–2209

Isambert H, Maggs A (1996) Dynamics and rheology of actin solutions. Macromolecules 29:1036–1040

Janmey PA, Leterrier JF, Herrmann H (2003) Assembly and structure of neurofilaments. Curr Opin Coll Int Sci 8:40–47

Kroy K, Frey E (1996) Force-extension relation and plateau modulus for wormlike chains. Phys Rev Lett 77:306–309

Kumar S, Hoh J (2004) Modulation of repulsive forces between neurofilaments by sidearm phosphorylation. Biochem Biophys Res Commun 324:489–496

Kumar S, Yin X, Trapp B, Hoh J, Paulaitis M (2002a) Relating interactions between neurofilaments to the structure of axonal neurofilament distributions through polymer brush models. Biophys J 82:2360–2372

Kumar S, Yin X, Trapp B, Paulaitis M, Hoh J (2002b) Role of long-range repulsive forces in organizing axonal neurofilament distributions: evidence from mice deficient in myelin-associated glycoprotein. J Neurosci Res 68:681–690

Langui D, Anderton BH, Brion JP, Ulrich J (1988) Effects of aluminum-chloride on cultured-cells from rat-brain hemispheres. Brain Res 438:67–76

Langui D, Probst A, Anderton B, Brion JP, Ulrich J (1990) Aluminum-induced tangles in cultured rat neurons—enhanced effect of aluminum by addition of maltol. Acta Neuropathol 80:649–655

Leterrier JF, Eyer J (1987) Properties of highly viscous gels formed by neurofilaments invitro—a possible consequence of a specific inter-filament cross-bridging. Biochem J 245:93–101

Leterrier JF, Langui D, Probst A, Ulrich J (1992) A molecular mechanism for the induction of neurofilament bundling by aluminum ions. J Neurochem 58:2060–2070

Leterrier J, Kas J, Hartwig J, Vegners R, Janmey PA (1996) Mechanical effects of neurofilament cross-bridges—modulation by phosphorylation, lipids, and interactions with F-actin. J Biol Chem 271:15687–15694

MacKintosh F, Kas J, Janmey PA (1995) Elasticity of semiflexible biopolymer networks. Phys Rev Lett 75:4425–4428

Meechai N, Jamieson AM, Blackwell J, Carrino DA, Bansal R (2001) Nonlinear viscoelasticity of concentrated solutions of aggrecan aggregate. Biomacromolecules 2:780–787

Meechai N, Jamieson AM, Blackwell J, Carrino DA, Bansal R (2002) Viscoelastic properties of aggrecan aggregate solutions: dependence on aggrecan concentration and ionic strength. J Rheol 46:685–707

Mukhopadhyay R, Kumar S, Hoh JH (2004) Molecular mechanisms for organizing the neuronal cytoskeleton. BioEssays 26:1017–1025

Pampaloni F, Lattanzi G, Jonas A, Surrey T, Frey E, Florin EL (2006) Thermal fluctuations of grafted microtubules provide evidence of a length-dependent persistence length. Proc Natl Acad Sci USA 103:10248–10253

Rubinstein M, Colby R (2004) Polymer physics. Oxford University Press, Oxford

Schilling J, Sackmann E, Bausch A (2004) Digital imaging processing for biophysical applications. Rev Sci Inst 75:2822–2827

Schmidt CF, Bärmann M, Isenberg G, Sackmann E (1989) Chain dynamics, mesh size and diffusive transport in networks of polymerized actin—a quasieleastic light scattering and microfluorescence study. Macromolecules 22:3638–3649

Semmrich C (2007) Nonlinear elasticity of pure F-actin solutions (in preparation)

Shea TB, Beermann ML (1994) Multiple interactions of aluminum with neurofilament subunits—regulation by phosphate-dependent interactions between C-terminal extensions of the high and middle molecular-weight subunits. J Neurosci Res 38:160–166

Tharmann R, Claessens MMAE, Bausch AR (2006) Micro- and macrorheological properties of actin networks effectively cross-linked by depletion forces. Biophys J 90:2622–2627

Tharmann R, Claessens MMAE, Bausch A (2007) Viscoelasticity of isotropically cross-linked actin networks. Phys Rev Lett 98:088103

Valentine M, Perlman ZE, Gardel ML, Shin JH, Matsudaira P, Mitchison TJ, Weitz DA (2004) Colloid surface chemistry critically affects multiple particle tracking measurements of biomaterials. Biophys J 86:4004–4014

Wilhelm J, Frey E (1996) Radial distribution function of semiflexible polymers. Phys Rev Lett 77:2581–2584